INTERNATIONAL JOURNAL OF OPTIMIZATION IN CIVIL ENGINEERING
Int. J. Optim. Civil Eng., 2017; 7(3)319-338

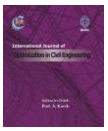

MULTI-OBJECTIVE SEMI-ACTIVE BASE ISOLATION SYSTEM

M. Mohebbi[*, †] and H. Dadkhah
Faculty of Engineering, University of Mohaghegh Ardabili, 56199-11367, Ardabil, Iran

ABSTRACT

Semi-active base isolation system has been proposed mainly to mitigate the base drift of isolated structures while in most cases, its application causes the maximum acceleration of superstructure to be increased. In this paper, designing optimal semi-active base isolation system composed of linear base isolation system with low damping and magneto-rheological (MR) damper has been studied for controlling superstructure acceleration and base drift separately and simultaneously. A multi-objective optimization problem has been defined for optimal design of semi-active base isolation system which considers a linear combination of maximum acceleration and base drift as objective function where Genetic algorithm (GA) has been used to solve the optimization problem. H_2/Linear Quadratic Gaussian (LQG) and clipped-optimal control algorithms have been used to determine the desired control force and the voltage of MR damper in each time step. For numerical simulation, a four-story base isolated shear frame has been considered and for different values of weighting parameter in objective function, optimal semi-active base isolation system has been designed under various design earthquakes. The results show that by using base isolation system and supplemental MR damper, the superstructure acceleration and base drift can be suppressed significantly. Also, it has been concluded that by selecting proper values for maximum acceleration and base drift related weighting parameters in objective function, it is possible to mitigate the maximum acceleration and base drift simultaneously. Furthermore, semi-active control system has worked successfully under testing earthquakes regarding design criteria.

Keywords: semi-active base isolation; MR damper; clipped-optimal control; genetic algorithm.

Received: 20 September 2016; Accepted: 10 January 2017

[*]Corresponding author: Faculty of Engineering, University of Mohaghegh Ardabili, 56199-11367. Ardabil, Iran
[†]E-mail address: mohebbi@uma.ac.ir (M. Mohebbi)

1. INTRODUCTION

Base isolation system is an effective control system which can reduce the response of structure significantly. Its utilization has mostly drawbacks such as high base drift and no adapting to different conditions. Base isolation system mitigates the structure response by shifting the period of structure. To this end, the stiffness of base isolation system is selected less than the structure stiffness which this low stiffness causes the high base drift. Also, because the base isolation system is a passive control system, it cannot be adopted to different earthquakes. To overcome these drawbacks, base isolation is used in combination with passive [1], semi-active [2] and active [3-5] control systems. Though adding supplemental passive control system can reduce the base drift, this hybrid control system cannot be adopted to different conditions because its behavior is constant during excitation. Using semi-active and active control systems lead to the adaptive hybrid system to different earthquakes in addition to reduction of base drift. However, active control systems need high external power supply during excitation that limits their application while semi-active control systems can operate with low external power supply. So, semi-active control systems are proper selection to combine with base isolation system. Different semi-active control systems have been studied as supplemental system of base isolation such as variable orifice damper [6-8] and variable friction system [2]. MR damper is another semi-active control system that has been widely used separately [9-14] or in combination with base isolation system [15-20]. Johnson et al. [15] demonstrated that adding MR damper to base isolation system can reduce the peak base drift. Yoshioka et al. [16] investigated the performance of semi-active base isolation system under far-field and near-field earthquakes and showed its effectiveness for both earthquakes. Lee et al. [19] employed clipped-optimal algorithm to apply voltage and showed that semi-active base isolation system can significantly reduce the structural response.

Dyke et al. [21] proposed H_2/LQG algorithm to determine the desired control force of MR damper. In H_2/LQG algorithm, the controller weighting parameter has been determined based on try and error in previous researches [21-22] or optimization procedure [23]. In application of semi-active base isolation system, the main objective from adding MR damper has been mitigating the base drift of isolated structure which in most case, it causes the superstructure acceleration to be increased. In previous researches, controlling the base drift and acceleration has not been investigated simultaneously, while increasing the maximum acceleration of superstructure causes problems regarding occupant comfort ability criterion. Hence in this paper, it has been decided to design semi-active base isolation system to mitigate the maximum base drift of base isolated structure and superstructure acceleration, simultaneously. To this end, a multi-objective function has been considered which includes the maximum acceleration and base drift in objective function to be minimized.

2. SEMI-ACTIVE BASE ISOLATION MODEL

According to the results of previous researches, it can be said that the structure response controlled by semi-active base isolation system falls in the linear region. Therefore, in this

paper it can be assumed that the structure has had the linear behavior. The equation of motion of isolated structure by semi-active base isolation system can be written as:

$$M_s\ddot{x}+C_s\dot{x}+K_s x=\Gamma f-M_s\Lambda\ddot{x}_g \tag{1}$$

where $\Gamma = [-1\ 0]^T$ indicates the location of MR damper that has been installed between base isolation and ground , Λ is a vector that all components are unity, f is MR damper force, $\ddot{x}_g$ is the ground acceleration, x is the vector of the displacements of the structure relative to the ground and M_s, K_s and C_s are the mass, stiffness and damping matrices of system. In this paper, a linear elastomeric with low damping is considered as base isolation system. To model base isolation system, one degree of freedom is added to the dynamic model of fixed base structure.

The state-space form of the equation of motion is given by:

$$\dot{Z}=AZ+Bf+E\ddot{x}_g \tag{2}$$

$$y=CZ+Df+\nu \tag{3}$$

where Z is the state vector ($Z=[x,\dot{x}]^T$), v is the measurement noise vector, y is the vector of measured outputs and A, B, C, D and E are system matrices.

MR damper behavior depends on the value of voltage current and can be adopted by changing voltage. The simple mechanical idealization of the MR damper is shown in Fig. 1 [21].

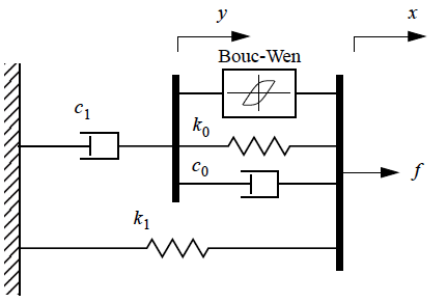

Figure 1. Simple mechanical model of the MR damper

The applied force predicted by this model is given as [21]:

$$f=az+c_0(\dot{x}-\dot{y})+k_0(x-y)+k_1(x-x_0) \tag{4}$$

or equivalently

$$f=c_1\dot{y}+k_1(x-x_0) \tag{5}$$

$$\dot{z}=-\gamma|\dot{x}-\dot{y}||z|^{n-1}-\beta(\dot{x}-\dot{y})|z|^n+A(\dot{x}-\dot{y}) \tag{6}$$

$$\dot{y} = \frac{1}{c_1 + c_0}\{az + c_0\dot{x} + k_0(x - y)\} \tag{7}$$

where k_1, c_0 and c_1 represent the accumulator stiffness, the viscous damping and dashpot, respectively. x_0 is the initial displacement of spring k_1, k_0 is present to control the stiffness at the large velocities and the parameters γ, β and A are the parameters used to define the shape of hysteresis loops.

Spencer et al. [24] have presented the following equations to determine the dynamic parameters of MR damper according to the applied voltage:

$$a = a(u) = a_a + a_b u \tag{8a}$$

$$c_1 = c_1(u) = c_{1a} + c_{1b} u \tag{8b}$$

$$c_0 = c_0(u) = c_{0a} + c_{0b} u \tag{8c}$$

where u is given as the output of a first-order filter given by:

$$\dot{u} = -\eta(u - V) \tag{9}$$

V is the value of voltage and η is constant modulus with dimension sec^{-1}.

3. CONTROL ALGORITHM

In this paper, clipped-optimal control algorithm is employed to determine the applied voltage to MR damper as [21]:

$$V = V_{\max} H\{(f_c - f) f\} \tag{10}$$

V_{max} is the maximum voltage that can be applied to MR damper, and $H\{.\}$ is the Heaviside step function. According to property of the Heaviside step function, it is clear that the applied voltage is set to zero or the maximum voltage. A block diagram of the clipped-optimal control is shown in Fig. 2. f_c is the desired control force that is determined by H_2/LQG control algorithm [21]. In this algorithm, $\ddot{x}_g$ is taken to be a stationary white noise and the structure response is minimized by using the following cost function:

$$J = \lim_{\tau \to \infty} \frac{1}{\tau} E[\int_0^{\tau} (z^T(t) Q z(t) + r f_c^2) dt] \tag{11}$$

where Q and r are the controller weighting matrix and parameter which affect the performance of control system.

In this paper, the controller weighting matrix Q is selected as unit matrix and the controller weighting parameter r is optimized by using genetic algorithm (GA) for different objective functions. Minimizing the cost function of Eq. (11) leads to the desired control

force as follow:

$$f_c = -k_c \bar{z} \tag{12}$$

$$\dot{\bar{z}} = A\bar{z} + Bf + L(y - C\bar{z} - Df) \tag{13}$$

k_c is the gain matrix for Linear Quadratic Regulator (LQR) and L is the gain matrix for state estimator which is determined as:

$$k_c = \frac{B'P}{r} \tag{14}$$

$$L = (CS)' \tag{15}$$

where P and S are the solution of the algebraic Ricatti equation given by:

$$PA + A'P - PB'BP/r + Q = 0 \tag{16}$$

$$SA' + AS - SC'CS + \gamma EE' = 0 \tag{17}$$

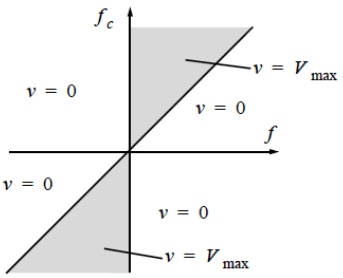

Figure 2. Diagram of clipped-optimal control algorithm

4. OPTIMAL DESIGN OF SEMI-ACTIVE BASE ISOLATION SYSTEM

In this paper, to improve the safety and occupant comfort ability design criteria, semi-active base isolation system is designed to reduce the maximum base drift and acceleration of superstructure, simultaneously. For this purpose, a multi-objective function optimization problem is defined to design the optimal semi-active base isolation system which considers a linear combination of maximum acceleration and base drift as objective function and the controller weighting parameter r as variable. Hence, the optimal value of controller weighting parameter is determined by solving the following optimization problem:

$$\text{Find: } X = r \tag{18}$$

$$\text{Minimize: } g_{\max} = \alpha \frac{\max(d_b)_{Semi-Active-B-I}}{\max(d_b)_{Single-B-I}} + \beta \frac{\max(a_1,...,a_4)_{Semi-Active-B-I}}{\max(a_1,...,a_4)_{Fixed-Base}} \tag{19}$$

where d_b and a_i are the base drift of isolated structure and floor acceleration of superstructure. α and β are weighting parameters which is applied on the peak base drift and acceleration. In Eq. (19), using different values for α and β leads to different reduction in the base drift and acceleration. It is clear that when α=1 and β=0, it is desired to minimize the maximum base drift and also by selecting α=0 and β=1, mitigating the maximum acceleration of superstructure has been important. To solve the optimization problem, genetic algorithm (GA) has been employed.

4.1 Genetic algorithms (GAs)

GA is a method for optimization of problems which uses principles inspired by natural genetics [25]. GA has been applied to solve the optimization problems in different fields of civil engineering such as optimal design of multiple tuned mass damper [26], optimal locations of the actuators for frame active control [27], solution of truss optimization problems [28] and stability analysis of gravity dams [29]. Fundamental parameters in the GA are: (1) chromosome representation, (2) initial population, (3) fitness function, (4) selection function, (5) crossover, (6) mutation.

(1)Chromosome representation

A GA starts with a population of chromosomes and goes toward better chromosome in next generation. Each chromosome is created from a sequence of genes and represented in real-valued or binary coding. In this research real-valued coding has been applied for chromosomes representation.

(2)Initial population

The GA requires an initial population to solve the optimization problem that is created by a random number generator. The total number of chromosome in each population called population size is important in the optimization problems. A high population size will result a large computational cost while a low population size will cause to inadequate computational accuracy. The range of 50-150 population size has been proposed to balance between computational cost and accuracy [30]. In this study, the population size is set to 50 chromosomes.

(3)Fitness function

The fitness value of chromosomes is effective factor in selection of chromosomes for mating. In this paper, the fitness function is defined the rank of each chromosome in the sorted objective function.

(4)Selection function

The selection function is employed to select the chromosomes from current generation for crossover. In this research, the stochastic universal sampling method [31] has been used for selection operator based on chromosome fitness value as:

$$P(x_i)=\frac{F(x_i)}{\sum_{i=1}^{N_{ind}}F(x_i)},i=1,2,...,N_{ind} \tag{20}$$

where $F(x_i)$ is the fitness value of chromosome x_i, $P(x_i)$ is probability of selection of x_i and N_{ind} is the population size.

(5)Crossover

The crossover operator is used to produce new chromosome from the parents. In this paper, the method proposed by Mühlenbein and Schlierkamp-Voosen [32] has been used for crossover. Two newborns are produced from each pair of parents that each newborn gets its genes from either parent with equal probability as follows:

$$O = P_2 + \alpha(P_2 - P_1) \tag{21}$$

where P_1 and P_2 are the parent genes, O is the newborn gene, and α is a scale factor selected randomly between [-0.25,1.25].

(6)Mutation

In GA, the mutation operator helps GA to escape from the local optimum. This operator alters the genes of a chromosome and produces a newborn. The mutation ratio shows the number of parents selected for mutation. In this paper, mutation rate=4% has been selected and also the Gaussian mutation is employed for mutation operator [33].

In this research, the elite strategy has been used where a number of the best chromosomes are selected as elites and go to the next generation directly.

5. NUMERICAL EXAMPLE

For numerical simulations, a four-story shear building has been considered to evaluate the performance of semi-active base isolation system. The properties of isolated structure have been presented in Table 1 [34].

Table 1: Parameters of structure and base isolation

Story	Floor masses (*ton*)	Stiffness coefficients (*MN/m*)	Damping coefficients (*KN.s/m*)
Base isolation	450	18.05	26.17
1	345	340	490
2	345	326	467
3	345	285	410
4	345	250	350

By defining y in Eq. (3) as $y = [\ddot{x}_b, \ddot{x}_1, \ddot{x}_2, \ddot{x}_3, \ddot{x}_4, x_b]$ which includes the structure accelerations and the base drift, the system matrices A, B, C, D and E in Eq.s (2) and (3) can be written as:

$$A = \begin{bmatrix} 0_{5\times5} & I_{5\times5} \\ -M_s^{-1}K_s & -M_s^{-1}C_s \end{bmatrix},\ B = \begin{bmatrix} 0_{5\times1} \\ M_s^{-1}\Gamma \end{bmatrix},\ E = \begin{bmatrix} 0_{5\times1} \\ \Lambda_{5\times1} \end{bmatrix},$$

$$C = \begin{bmatrix} -M_s^{-1}K_s & -M_s^{-1}C_s \\ 1,0_{1\times4} & 0_{1\times5} \end{bmatrix},\ D = \begin{bmatrix} M_s^{-1}\Gamma \\ 0 \end{bmatrix},$$

The dynamical parameters of MR damper used in this paper have been reported in Table 2 [22]. The capacity and maximum voltage of MR damper have been 1000 (*kN*) and 10 (*v*), respectively.

Table 2: Parameters of MR damper model

Parameter	Value	Parameter	Value
c_{0a}	110 *kN.sec/m*	a_a	46.2 *kN/m*
c_{0b}	114.3 *kN.sec/m.V*	a_b	41.2 *kN/m.V*
k_0	0.002 *kN/m*	γ	164 m^{-2}
c_{1a}	8359.2 *kN.sec/m*	β	164 m^{-2}
c_{1b}	7482.9 *kN.sec/m.V*	A	1107.2
k_1	0.0097 *kN/m*	n	2
x_0	0	η	100 sec^{-1}

For numerical simulation, a program has been developed by using MATLAB software which in this program, the MR damper behavior has been controlled by using H_2/LQG and clipped-optimal control algorithms and also the matrix of k_c in Eq. (14) has been calculated by using the control toolbox in MATLAB. The comparison of results of this program and experimental study produced by Dyke et al. [21] shows its acceptable accuracy. This research includes the following sections:

(a): designing passive hybrid base isolation system

(b): designing optimal semi-active base isolation system

(c): assessment of semi-active base isolation performance under testing earthquakes

5.1 (a): Designing passive hybrid base isolation system

MR damper can be employed with the constant voltage that operates the same as passive control system. In this section, the performance of hybrid base isolation system is studied in passive form and the structure response is evaluated for the constant voltages of 0, 5 and 10 (v). The peak response of structure subjected to El Centro (PGA=0.348g, 1940), Parkfield (PGA=0.35g, 1996) and Northridge (PGA=0.535g, 1994) earthquakes have been shown for the fixed-base structure and isolated structures by using single and passive hybrid base isolation systems in Tables 3-5 where d_b and d_i are drift of base isolation and the inter-story drift of superstructure, a_b and a_i are acceleration of base isolation and superstructure.

According to the results presented in Tables 3-5, it can be concluded that:

1) Isolating structure by using single base isolation system can mitigate the inter-story drift and acceleration which in this case study, the maximum inter-story drift has reduced about 66%, 88%, 80% and the maximum acceleration has reduced about 78, 88, 87% under El Centro, Parkfield and Northridge earthquakes, respectively. Therefore, single base isolation system is an effective control system in reducing structure response while the peak base drift has been high which in this research has been controlled by using MR damper.
2) Adding supplemental MR damper in passive form (constant voltage) can reduce the peak base drift effectively. This reduction is significant especially when the maximum voltage (*v=10*) has been applied. In this case, the peak base drift has reduced about 78%, 71% and

63% under El Centro, Parkfield and Northridge earthquakes, respectively. Therefore, using MR damper is an appropriate alternative for mitigating the maximum base drift.

3) Adding supplemental MR damper has reduced the structure response in comparison with single base isolation system under El Centro earthquake while it has increased the structure response under Parkfield and Northridge earthquakes. However, in comparison with fixed-base structure, under all excitations it has been seen that the response of superstructure has been suppressed significantly.
4) Increasing the voltage of MR damper has led to more reduction in the peak base drift while it increases mostly the peak inter-story drift and acceleration of superstructure. From the results of numerical simulations, it is clear that the minimum acceleration and base drift have been achieved by using passive-off (*v=0*) and passive-on (*v=10*) MR dampers, respectively.

Table 3: The peak response of structure subjected to El Centro earthquake

Response	Fixed base	Single base isolation	Hybrid base isolation (v=0)	Hybrid base isolation (v=5)	Hybrid base isolation (v=10)
d_b	-	31.53	19.15	9.46	6.94
d_1	3.88	1.30	0.80	0.54	0.59
d_2	3.52	1.04	0.63	0.47	0.59
d_3	3.09	0.81	0.49	0.38	0.53
d_4	2.08	0.47	0.28	0.27	0.43
(cm)					
a_b	-	286	183	161	253
a_1	722	302	193	132	224
a_2	1037	318	197	141	202
a_3	1165	329	200	161	225
a_4	1509	338	206	195	310
(cm/s^2)					
f (kN)	-	-	163.8	680.0	1000

Table 4: The peak response of structure subjected to Parkfield earthquake

Response	Fixed base	Single base isolation	Hybrid base isolation (v=0)	Hybrid base isolation (v=5)	Hybrid base isolation (v=10)
d_b	-	5.77	3.41	2.14	1.66
d_1	1.87	0.23	0.17	0.33	0.50
d_2	1.76	0.20	0.17	0.42	0.61
d_3	1.70	0.19	0.17	0.44	0.64
d_4	1.08	0.13	0.13	0.34	0.57
(cm)					
a_b	-	82	75	158	276
a_1	239	63	49	162	210
a_2	452	59	40	107	190
a_3	619	63	56	189	268
a_4	786	93	91	244	418
(cm/s^2)					
f (kN)	-	-	110.1	583.0	1000

Table 5: The peak response of structure subjected to Northridge earthquake

Response	Fixed base	Single base isolation	Hybrid base isolation (v=0)	Hybrid base isolation (v=5)	Hybrid base isolation (v=10)
d_b	-	11.12	10.65	4.66	4.16
d_1	2.28	0.45	0.46	0.33	0.45
d_2	2.10	0.36	0.38	0.32	0.41
d_3	1.90	0.28	0.31	0.35	0.52
d_4	1.25	0.16	0.18	0.30	0.38
(cm)					
a_b	-	108	120	168	284
a_1	550	110	115	145	255
a_2	642	110	115	181	291
a_3	679	114	121	148	316
a_4	907	116	133	216	278
(cm/s^2)					
$f\,(kN)$	-	-	125.6	581.3	1000

5.2 (b): Designing optimal semi-active base isolation system

To assess the effect of controller weighting parameter, r, in Eq. (11) on the performance of semi-active base isolation system in controlling the maximum base drift and superstructure response, for different values of r , the maximum response of controlled system has been determined and given in Tables 6-8.

Table 6: The maximum response of controlled structure under El Centro earthquake

r	10^{-10}	10^{-14}	10^{-18}	10^{-22}	10^{-26}
d_b	19.13	7.32	6.86	6.85	6.86
d_1	0.80	0.53	0.56	0.57	0.57
d_2	0.63	0.46	0.48	0.48	0.48
d_3	0.49	0.41	0.42	0.41	0.41
d_4	0.28	0.31	0.34	034	0.34
(cm)					
a_b	183	156	153	154	153
a_1	192	186	173	171	173
a_2	197	149	149	149	149
a_3	201	185	174	172	175
a_4	206	224	246	247	248
(cm/s^2)					
$f\,(kN)$	163.5	1000	1000	1000	1000

Table 7: The maximum response of controlled structure under Parkfield earthquake

r	10^{-10}	10^{-14}	10^{-18}	10^{-22}	10^{-26}
d_b	3.40	1.68	1.46	1.46	1.46
d_1	0.17	0.38	0.40	0.40	0.40
d_2	0.17	0.48	0.52	0.52	0.52
d_3	0.16	0.50	0.53	0.53	0.53
d_4	0.12	0.45	0.47	0.47	0.47
(cm)					
a_b	74	230	244	244	244
a_1	50	184	188	188	188
a_2	41	115	136	136	136
a_3	57	218	205	205	206
a_4	90	327	343	343	342
(cm/s^2)					
$f\,(kN)$	110.2	969.3	1000	1000	1000

Table 8: The maximum response of controlled structure under Northridge earthquake

r	10^{-10}	10^{-14}	10^{-18}	10^{-22}	10^{-26}
d_b	10.66	3.97	3.64	3.64	3.65
d_1	0.46	0.37	0.36	0.36	0.36
d_2	0.38	0.37	0.36	0.36	0.36
d_3	0.31	0.34	0.31	0.31	0.31
d_4	0.18	0.21	0.20	0.20	0.20
(cm)					
a_b	120	137	129	146	145
a_1	115	106	118	119	119
a_2	115	107	101	104	107
a_3	121	132	132	130	132
a_4	133	151	143	143	144
(cm/s^2)					
$f\,(kN)$	125.6	1000	1000	1000	1000

As shown in Tables 6-8, under all excitations the performance of semi-active base isolation system depends on the value of controller weighting parameter. Moreover, according to the results it can be concluded that using large values for controller weighting parameter causes to have smaller peak acceleration and MR damper force in expense of larger base drift. Therefore, designing semi-active base isolation system for minimizing the maximum base drift leads to increase the maximum superstructure acceleration, consequently making problem in comfort ability of occupants. Therefore, to improve the safety and comfort ability design criteria simultaneously, it is recommended to mitigate the maximum drift and acceleration simultaneously. For this reason, in this paper for designing optimal semi-active control system, a multi-objective function has been used. To avoid from complexity in numerical simulations, the objective function has been defined as a linear combination of maximum normalized base drift and acceleration for each excitation as follows:

$$g_{\max_{El-Centro}} = \alpha \frac{\max(d_b)_{Semi-Active-B-I}}{31.53} + \beta \frac{\max(a_1,\ldots,a_4)_{Semi-Active-B-I}}{1509} \quad (22)$$

$$g_{\max_{Parkfield-California}} = \alpha \frac{\max(d_b)_{Semi-Active-B-I}}{5.77} + \beta \frac{\max(a_1,\ldots,a_4)_{Semi-Active-B-I}}{786} \quad (23)$$

$$g_{\max_{Northridge}} = \alpha \frac{\max(d_b)_{Semi-Active-B-I}}{11.12} + \beta \frac{\max(a_1,\ldots,a_4)_{Semi-Active-B-I}}{907} \quad (24)$$

The objective function has been solved for several combinations of α and β by using GA. For example, the variations of the best fitness, mean of fitness of individual and the average distance between individuals have been reported during generations in Fig. 3 for three weighting combinations of [α,β] under Parkfield earthquake. The convergence behavior of GA can be concluded from these results.

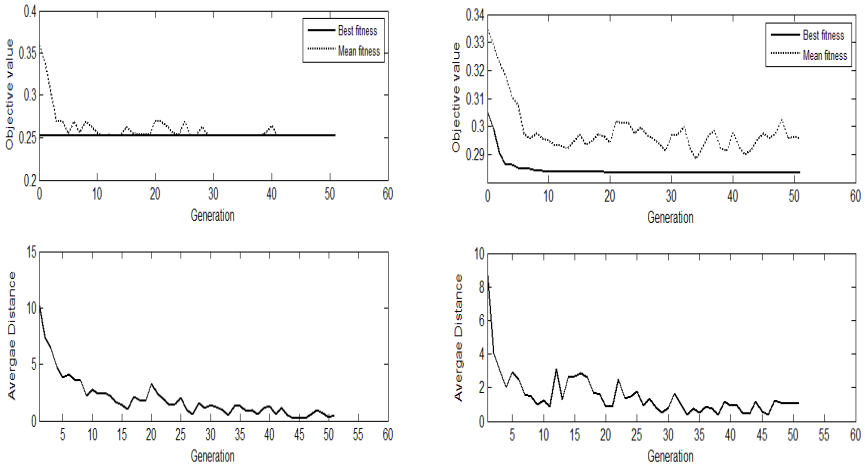

(a): [α,β]=[1,0] (b): [α,β]=[0.4,0.6]

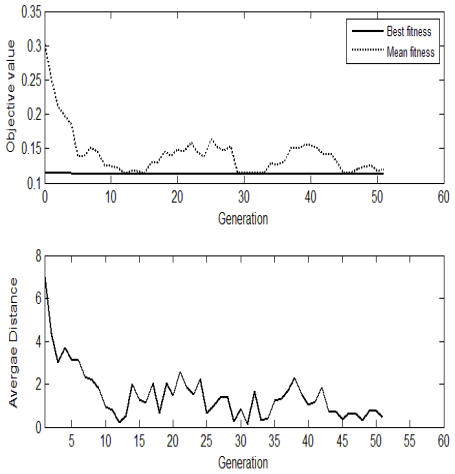

(c): [α,β]=[0,1]

Figure 3. Objective value and average distance between individuals under Parkfield earthquake

The maximum response of superstructure and base drift for different combinations of [α,β] as well as the optimum value for controller weighting parameter, r, have been reported in Tables 9-11.

Table 9: The maximum response for different combinations of α and β under El Centro earthquake

[α,β]	[1,0]	[0.8,0.2]	[0.6,0.4]	[0.5,0.5]	[0.4,0.6]	[0.2,0.8]	[0,1]
Optimal r	$10^{-18.838}$	$10^{-18.004}$	$10^{-13.686}$	$10^{-13.608}$	$10^{-13.608}$	$10^{-12.723}$	$10^{-12.271}$
d_b	6.84	6.85	7.41	7.45	7.45	9.21	11.56
d_1	0.57	0.56	0.53	0.52	0.52	0.56	0.59
d_2	0.48	0.48	0.47	0.45	0.45	0.46	0.47
d_3	0.42	0.42	0.39	0.40	0.40	0.36	0.37
d_4 (cm)	0.35	0.34	0.28	0.27	0.27	0.23	0.22
a_b	154	154	143	143	143	139	146
a_1	171	171	190	190	190	157	146
a_2	152	149	156	156	156	133	145
a_3	172	172	190	187	187	152	153
a_4 (cm/s^2)	251	246	201	199	199	165	158
f (kN)	1000	1000	1000	1000	1000	1000	1000

Table 10: The maximum response for different combinations of α and β under Parkfield earthquake

[α,β]	[1,0]	[0.8,0.2]	[0.6,0.4]	[0.5,0.5]	[0.4,0.6]	[0.2,0.8]	[0,1]
Optimal r	$10^{-19.401}$	$10^{-20.282}$	$10^{-18.849}$	$10^{-11.663}$	$10^{-11.427}$	$10^{-10.646}$	$10^{-10.646}$
d_b	1.46	1.46	1.46	2.72	2.90	3.40	3.40
d_1	0.40	0.40	0.40	0.21	0.19	0.17	0.17
d_2	0.52	0.52	0.52	0.23	0.21	0.17	0.17
d_3	0.53	0.53	0.53	0.21	0.19	0.16	0.16
d_4 (cm)	0.47	0.47	0.47	0.18	0.15	0.12	0.12
a_b	244	244	243	93	84	73	73
a_1	188	188	188	64	60	51	51
a_2	134	135	134	52	50	42	42
a_3	206	206	206	85	75	57	57
a_4 (cm/s^2)	343	342	342	131	109	89	89
f (kN)	1000	1000	1000	346.2	253.8	123.5	123.5

Table 11: The maximum response for different combinations of α and β under Northridge earthquake

$[\alpha,\beta]$	[1,0]	[0.8,0.2]	[0.6,0.4]	[0.5,0.5]	[0.4,0.6]	[0.2,0.8]	[0,1]
Optimal r	$10^{-19.078}$	$10^{-19.881}$	$10^{-20.368}$	$10^{-19.889}$	$10^{-16.282}$	$10^{-16.069}$	$10^{-12.335}$
d_b	3.62	3.64	3.63	3.64	3.68	3.70	7.34
d_1	0.36	0.36	0.36	0.36	0.36	0.36	0.35
d_2	0.36	0.36	0.36	0.36	0.36	0.36	0.30
d_3	0.31	0.31	0.31	0.31	0.32	0.32	0.27
d_4	0.20	0.20	0.20	0.20	0.19	0.19	0.16
(cm)							
a_b	131	144	144	144	130	130	123
a_1	119	119	118	119	118	117	99
a_2	108	105	106	105	98	97	97
a_3	130	130	130	130	134	135	107
a_4	144	142	141	142	139	139	120
(cm/s^2)							
f (kN)	1000	1000	1000	1000	1000	1000	741.4

Based on the results reported in Tables 9-11, it can be concluded that:

(1) Optimum controller weighting parameter, r, depends on the objective function. For example when $[\alpha,\beta]$ is equal to [1,0], it means that the objective function has been defined to minimize the peak base drift, the optimal controller weighting parameter under El Centro earthquake has been $r= 10^{-18.838}$ while for $[\alpha,\beta]$=[0,1] that the objective function has been minimizing the peak acceleration, optimal controller weighting parameter $r= 10^{-12.271}$ has been obtained.

(2) Using different values for α and β affects the performance of optimal semi-active base isolation system in controlling the maximum base drift and acceleration. Selecting $[\alpha,\beta]$= [1,0] and $[\alpha,\beta]$=[0,1] are threshold values which lead to maximum reduction in maximum base drift and acceleration, respectively. Hence based on the importance of reduction in base drift and acceleration, a proper set should be considered for $[\alpha,\beta]$.

Figs. 4-6 show the time history of structure response, MR damper force and voltage for three combinations of $[\alpha,\beta]$ under Northridge earthquake.

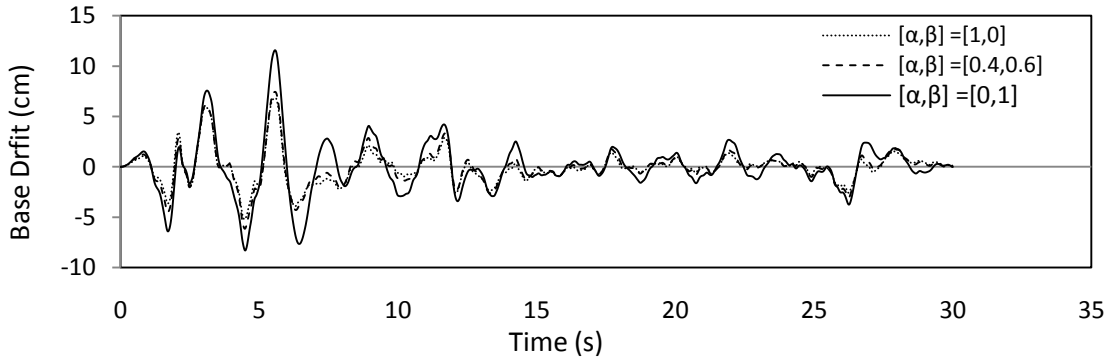

(a): Base drift

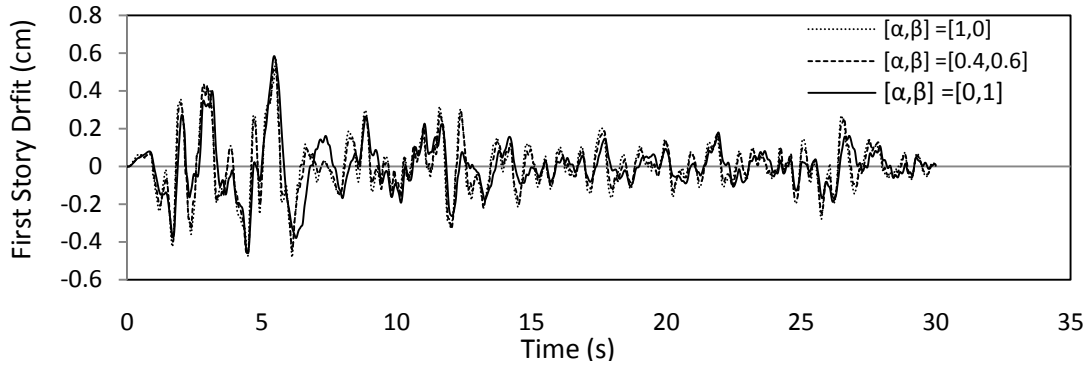

(b): Maximum inter-story drift

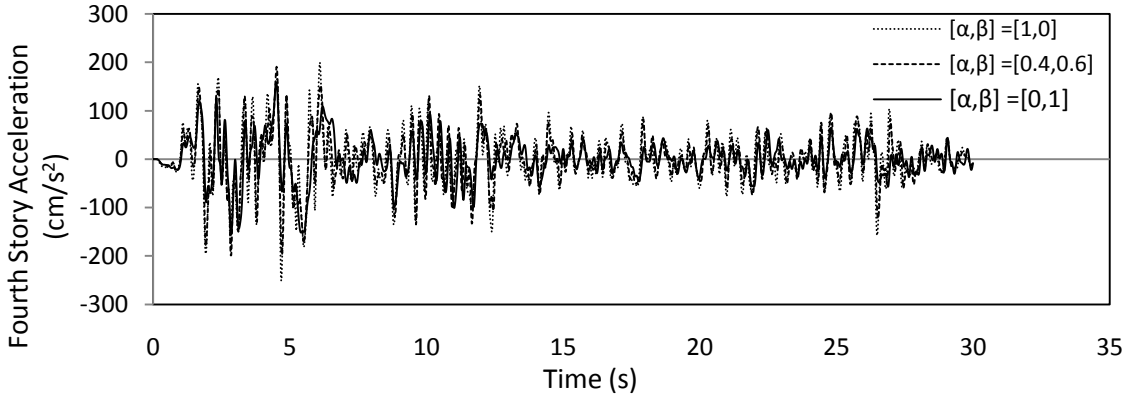

(c): Maximum acceleration

Figure 4. Time history of (a) base drift, (b) maximum inter-story drift, and (c) maximum acceleration

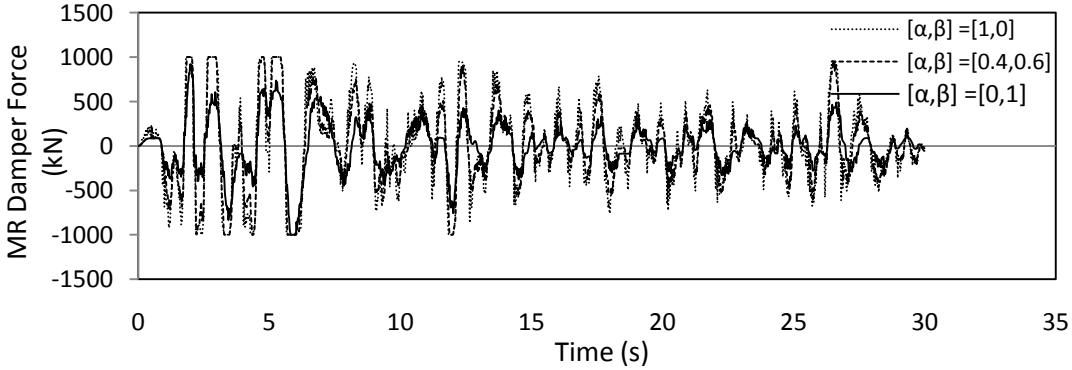

Figure 5. MR damper force

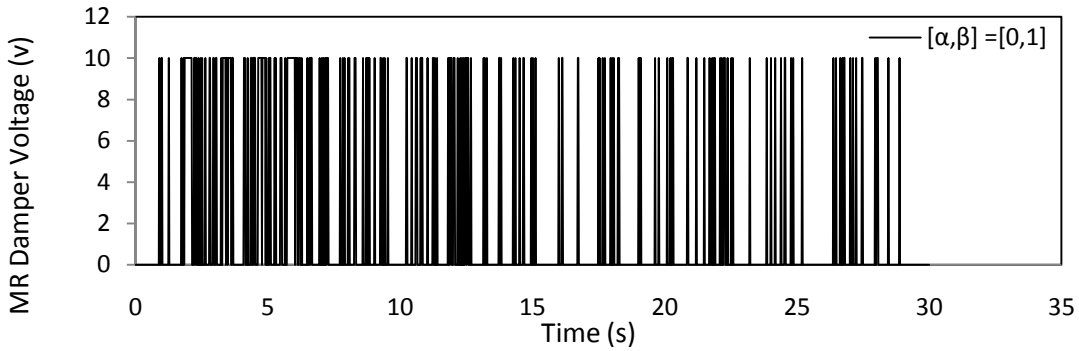

Figure 6. MR damper voltage

5.3 (c): Assessment of semi-active base isolation performance under testing earthquakes

In previous section, the semi-active base isolation system was designed when the structure subjected to a specific earthquake while earthquake is an unpredictable event and to check the reliability of control system, the performance of optimal designed control system should be evaluated under other earthquakes. To this end, the performance of designed control system is evaluated under Olympia (PGA=0.344g, 1994), Loma Prieta (PGA=0.278g, 1989) and Taft (PGA=0.18g, 1952) real earthquakes. For each combinations of [α,β], the logarithmical average of controller weighting parameter, r, under three design records has been used as the controller weighting parameter of semi-active control system under testing records. For different sets of [α,β], the maximum response of uncontrolled and controlled structures under testing excitations has been reported in Tables 12-14.

Table 12: The maximum responses of uncontrolled and controlled structures subjected to Olympia earthquake

Response	Fixed base	Single base isolation	Semi active base isolation		
			[α,β]=[1,0]	[α,β]=[0.2,0.8]	[α,β]=[0,1]
d_b	-	18.52	2.58	4.01	7.95
d_1	3.38	0.81	0.44	0.42	0.40
d_2	3.05	0.68	0.49	0.42	0.36
d_3	2.89	0.56	0.49	0.41	0.30
d_4	1.93	0.34	0.32	0.28	0.18
(cm)					
a_b	-	197	202	159	121
a_1	507	187	136	123	115
a_2	785	186	104	109	102
a_3	1013	218	179	138	116
a_4	1399	244	228	205	131
(cm/s^2)					
f (kN)	-	-	1000	991.4	484.6

Table 13: The peak responses of uncontrolled and controlled structures subjected to Loma Prieta earthquake

Response	Fixed base	Single base isolation	Semi active base isolation		
			$[\alpha,\beta]=[1,0]$	$[\alpha,\beta]=[0.2,0.8]$	$[\alpha,\beta]=[0,1]$
d_b	-	21.29	9.03	9.18	10.59
d_1	5.30	0.86	0.56	0.55	0.52
d_2	4.92	0.68	0.51	0.48	0.43
d_3	4.27	0.52	0.41	0.46	0.35
d_4	2.66	0.30	0.28	0.28	0.23
(cm)					
a_b	-	208	199	182	127
a_1	698	213	172	184	126
a_2	1134	213	172	175	137
a_3	1612	214	186	180	159
a_4	1927	220	202	202	164
(cm/s^2)					
$f\,(kN)$	-	-	1000	1000	818.6

Table 14: The peak responses of uncontrolled and controlled structures subjected to Taft earthquake

Response	Fixed base	Single base isolation	Semi active base isolation		
			$[\alpha,\beta]=[1,0]$	$[\alpha,\beta]=[0.2,0.8]$	$[\alpha,\beta]=[0,1]$
d_b	-	10.89	2.82	3.93	5.40
d_1	1.99	0.44	0.39	0.35	0.24
d_2	1.74	0.35	0.40	0.34	0.21
d_3	1.45	0.29	0.38	0.31	0.19
d_4	1.07	0.17	0.26	0.19	0.13
(cm)					
a_b	-	114	143	133	91
a_1	339	115	117	102	69
a_2	569	111	81	72	62
a_3	633	113	129	122	68
a_4	772	123	185	137	91
(cm/s^2)					
$f\,(kN)$	-	-	1000	961.9	439.2

The results show that the semi-active base isolation system has worked successfully under testing earthquakes, too, regarding the reduction achieved in maximum base drift and acceleration separately or simultaneously. Furthermore, for various sets of $[\alpha,\beta]$, the same trend in controlling the response of structure under design records has been obtained when the structure subjected to testing excitations.

6. CONCLUSIONS

In this paper, semi-active base isolation system composed of linear base isolation system with low damping and magneto rheological (MR) damper has been designed optimally. In designing procedure to improve the safety and occupant comfort ability design criteria, minimizing the peak base drift of isolated structure and the maximum acceleration of main structure, separately or simultaneously, have been selected as design objectives. For this end, a multi-objective optimization problem has been defined to design optimal semi-active base isolation system which considers an objective function as a linear combination of maximum acceleration and base drift. H_2/linear quadratic Gaussian (LQG) and clipped-optimal control algorithms have been used to determine the desired control force and applied voltage of MR damper in each time step. Genetic algorithm (GA) has been used to solve the optimization problem for different sets of weighting parameters assigned to acceleration and base drift in objective function. For numerical simulation, a four-story base isolated shear frame has been considered and the semi-active base isolation system has been designed optimally under different design earthquakes. Results show that the performance of semi-active base isolation system depends on the value of controller weighting parameter strongly and the superstructure response and base drift can be reduced by using the semi-active base isolation system significantly. Moreover, by selecting proper values for maximum acceleration and base drift related parameters in objective function, it is possible to mitigate the maximum acceleration and base drift to a desired level. For the case study of this research, when the weighting parameters of objective function have been selected in accordance with controlling only base drift or acceleration separately, the averages of reduction values under three design records have been 73% and 89% for base drift and acceleration, respectively, while in minimizing the base drift and acceleration simultaneously by using multi-objective optimization design procedure, the corresponding values have been about 65% and 85%. Evaluating the performance of designed optimal control system under testing earthquakes shows that the semi-active control system designed according to proposed multi-objective based design procedure, can satisfy the design objective under testing earthquakes.

REFERENCES

1. Constantinou MC, Symans MD, Tsopelas P, Taylor DP. Fluid dampers for application of seismic energy dissipation and seismic isolation, *Proceedings of the ATC-17-1 Seminar on Seismic Isolation, Passive Energy Dissipation and Active Control*, 1999.
2. Narasimhan S, Nagarajaiah S. Smart base isolated buildings with variable friction systems: H∞ controller and SAIVF device, *Earthq Eng Struct Dyn* 2006; **35**(8): 921-42.
3. Inaudi JA, Kelly JM. Hybrid isolation systems for equipment protection, *Earthq Eng Struct Dyn* 1993; **22**(4): 297-313.
4. Yang JN, Wu JC, Reinhorn AM, Riley M. Control of sliding-isolated buildings using sliding-mode control, *J Struct Eng* 1996; **122**(2): 179-86.
5. Nagarajaiah S, Riley MA, Reinhorn A. Control of sliding-isolated bridge with absolute acceleration feedback, *J Eng Mech* 1993; **119**(11): 2317-32.

6. Madden GJ, Symans MD, Wongprasert N. Experimental verification of seismic response of building frame with adaptive sliding base-isolation system, *J Struct Eng* 2002; **128**(8): 1037-45.
7. Wongprasert N, Symans MD. Experimental evaluation of adaptive elastomeric base-isolated structures using variable-orifice fluid dampers, *J Struct Eng* 2005; **131**(6): 867-77.
8. Wongprasert N, Symans MD. Numerical evaluation of adaptive base-isolated structures subjected to earthquake ground motions, *J Eng Mech* 2005; **131**(2): 109-19.
9. Li Z, Chang CC, Spencer BF. Intelligent technology-based control of motion and vibration using MR dampers, *Earthq Eng Eng Vib* 2002; **1**(1): 100-10.
10. Jing C, Youlin X, Weilian Q, Zhilun W. Seismic response control of a complex structure using multiple MR dampers: experimental investigation, *Earthq Eng Eng Vib* 2004; **3**(2): 181-93.
11. Choi KM, Lee HJ, Cho SW, Lee IW. Modified energy dissipation algorithm for seismic structures using magnetorheological damper, *KSCE J Civil Eng* 2007; **11**(2): 121-26.
12. Moon SJ, Huh YC, Jung HJ, Jang DD, Lee HJ. Sub-optimal design procedure of valve-mode magnetorheological fluid dampers for structural control, *KSCE J Civil Eng* 2011; **15**(5): 867-73.
13. Bharti SD, Dumne SM, Shrimali MK. Earthquake response of asymmetric building with MR damper, *Earthq Eng Eng Vib* 2014; **13**(2): 305-16.
14. Cho SW, Jung HJ, Lee IW. Smart passive system based on magnetorheological damper, *Smart Mater Struct* 2005; **14**(4): 707-14.
15. Johnson EA, Ramallo JC, Spencer BF, Sain MK. Intelligent base isolation systems, *Proceedings of the 2nd World Conference on Structural Control, Kyoto, Japan* 1999, **1**: pp. 367–376.
16. Yoshioka H, Ramallo JC, Spencer BF. Smart base isolation strategies employing magnetorheological dampers, *J Eng Mech* 2002; **128**(5): 540-51.
17. Ramallo JC, Johnson EA, Spencer BF. Smart base isolation systems, *J Eng Mech* 2002; **128**(10): 1088-99.
18. Sahasrabudhe S, Nagarajaiah S. Experimental study of sliding base-isolation buildings with magneto-rheological dampers in near-fault earthquake, *J Struct Eng* 2005; **131**(7): 1025-34.
19. Lee HJ, Yang G, Hung HJ, Spencer BF, Lee IW. Semi-active neurocontrol of a base-isolated benchmark structure, *Struct Cont Health Monitor* 2006; **13**(2): 682-92.
20. Ali SF, Ramaswamy A. Hybrid structural control using magnetorheological dampers for base isolated structures, *Smart Mater Struct* 2009; **18**(5): 055011.
21. Dyke SJ, Spencer BF, Sain MK, Carlson JD. Modeling and control of magnetorheological dampers for seismic response reduction, *Smart Mater Struct* 1996; **5**(5): 565-75.
22. Mohajer Rahbari N, Farahmand Azar B, Talatahari S, Safari H. Semi-active direct control method for seismic alleviation of structures using MR dampers, *Struct Cont Health Monito* 2013; **20**(6): 1021-42.
23. Mohebbi M, Dadkhah H, Shakeri K. Optimal hybrid base isolation and MR damper, *Int J Optim Civil Eng* 2015; **5**(4): 493-509.
24. Spencer BF, Dyke SJ, Sain MK, Carlson JD. Phenomenological model for magnetorheological dampers, *J Eng Mech* 1997; **123**(3): 230-8.
25. Gómez-Skarmeta AF, Jiménez F. Fuzzy modeling with hybrid systems, *Fuzzy Set Syst* 1999; **104**(2): 199-208.
26. Mohebbi M. Minimizing Hankel's Norm as Design Criterion of Multiple Tuned Mass Dampers, *Int J Optimization Civil Eng* 2013; **3**(2): 271-88.

27. Rezaiee-Pajand M, Payandeh Sani M. Three schemes for active control of the planar frame, *Int J Optim Civil Eng* 2015; **5**(1): 117-35.
28. Salar M, Ghasemi MR, Dizangian B. A fast GA-based method for solving truss optimization problems, *Int J Optim Civil Eng* 2016; **6**(1): 101-14.
29. Haghighi A, Ayati AH. Uncertainty analysis of stability of gravity dams using the fuzzy set theory, *Int J Opt Civil Eng* 2015; **5**(4): 465-78.
30. Pham DT, Karaboga D. *Intelligent Optimisation Techniques: Genetic Algorithms, Tabu Search, Simulated Annealing Aand Neural Networks*, Springer, London, 2012.
31. Baker JE. Reducing bias and inefficiency in the selection algorithm, *Proceedings of the 2nd International Conference on Genetic Algorithm (ICGA), Cambridge, MA, USA* 1987; pp. 14-21.
32. Muhlenbein H, Schlierkamp-Voosen D. Predictive models for the breeder genetic algorithm: I. continuous parameter optimization, *Evolut Comput* 1993; **1**(1): 25-49.
33. Dong H, He J, Huang H, Hou W. Evolutionary programming using a mixed mutation strategy, *Inform Sci* 2007; **177**(1): 312-27.
34. GÜÇLÜ R. Fuzzy logic control of vibrations of analytical multi-degree-of-freedom structural systems, *Turkish J Eng Environ Sci* 2003; **27**(3): 157-68.